Structure Study of Cellulose Fibers Wet-Spun from Environmentally Friendly NaOH/Urea Aqueous Solutions

Xuming Chen,[†] Christian Burger,[†] Fen Wan,[†] Jun Zhang,[†] Lixia Rong,[†] Benjamin S. Hsiao,*[,†] Benjamin Chu,*[,†] Jie Cai,[‡] and Lina Zhang[‡]

Department of Chemistry, Stony Brook University, Stony Brook, New York 11794−3400, and Department of Chemistry, Wuhan University, Wuhan 430072, China

Received December 14, 2006; Revised Manuscript Received March 23, 2007

In this study, structure changes of regenerated cellulose fibers wet-spun from a cotton linter pulp (degree of polymerization ~620) solution in an NaOH/urea solvent under different conditions were investigated by simultaneous synchrotron wide-angle X-ray diffraction (WAXD) and small-angle X-ray scattering (SAXS). WAXD results indicated that the increase in flow rate during spinning produced a better crystal orientation and a higher degree of crystallinity, whereas a 2-fold increase in draw ratio only affected the crystal orientation. When coagulated in a H_2SO_4/Na_2SO_4 aqueous solution at 15 °C, the regenerated fibers exhibited the highest crystallinity and a crystal orientation comparable to that of commercial rayon fibers by the viscose method. SAXS patterns exhibited a pair of meridional maxima in all regenerated cellulose fibers, indicating the existence of a lamellar structure. A fibrillar superstructure was observed only at higher flow rates (>20 m/min). The conformation of cellulose molecules in NaOH/urea aqueous solution was also investigated by static and dynamic light scattering. It was found that cellulose chains formed aggregates with a radius of gyration, R_g, of about 232 nm and an apparent hydrodynamic radius, R_h, of about 172 nm. The NaOH/urea solvent system is low-cost and environmentally friendly, which may offer an alternative route to replace more hazardous existing methods for the production of regenerated cellulose fibers.

Introduction

Developments of new bio-based products and related technologies have gained significant momentum over the past decade. Biopolymers from various natural resources such as cellulose, starch, and proteins have been considered as alternative materials to solve the widespread dependence on fossil fuel since they are abundant, renewable, eco-friendly, and biodegradable. According to the Technology Road Map for Plant/Crop-Based Renewable Resources 2020, sponsored by the U.S. Department of Energy (DOE), the application of plant-derived renewable resources may increase to 10% of the basic chemical building blocks by 2020, and to 50% by 2050.[1] Cellulose is the most abundant biological material on earth. It is estimated that between 10^{10} to 10^{11} tons of cellulose are globally synthesized and destroyed each year.[2] Regeneration of cellulose fibers is one of the most important tasks for the application of the native cellulose. Various methods are in use to regenerate cellulose fibers, such as the viscose, cuprammouniom, cellulose acetate, and Lyocell processes. The fraction of regenerated cellulose fibers in the global fiber market had been as high as 20% during the 1960s.[3] However, after the invention of many low-cost synthetic polymer fibers, especially polyamide and polyester fibers, the market for regenerated cellulose fibers has decreased steadily in the past decades. Nevertheless, the production of regenerated cellulose is still quite substantial today. For example, in 1998, 475 300 tons of viscose was produced in China, and it is forecast that China may produce 700 000 tons of viscose by 2010.[3] There were 156 viscose fiber plants in the world in 1998,[3] and based on the production of the plants in China, it can be estimated that more than 1 500 000 tons of viscose were produced in the world in 1998.

The environmental problem and the high cost have been two major issues affecting the production and application of regenerated cellulose fibers in recent years. The viscose process is the oldest technology for producing regenerated cellulose fibers (i.e., rayon fibers); it was developed over 100 years ago.[4] This process, unfortunately, uses or generates several environmentally hazardous chemicals, including CS_2, H_2S, and heavy metals.[5] The cuprammonium process is an alternative route to produce regenerated cellulose fibers (cupro silk, cuprophane). However, it also has its own environmental problems and has only been practiced scarcely in the industry.[4] Throughout the years, many other alternative methods have been demonstrated to reduce the processing steps as well as to minimize hazardous byproducts. For example, the *N*-methylmorpholine-*N*-oxide (NMMO, Lyocell) process has become a more desirable method over the popular viscose process because it involves less hazardous compounds. The NMMO process also includes the use of a cross-linking agent that binds the cellulose fibrils together, thereby simultaneously enhancing the transverse as well as the longitudinal properties.[6] However, the Lyocell process still has some environmental issues that need to be overcome for the efficient and environment-friendly regeneration of cellulose fibers, including the minimization of several side reactions, further reduction of undesired byproducts, and efficient recovery of the expensive solvent.[7]

It has been reported that the rayon fiber with its unique characteristics, for example, biodegradability and biocompatibility, has the potential to become the leading fiber used in the fiber industry, if the inherent pollution problems associated

* To whom correspondence should be addressed. Tel.: (631) 632-7793 (B.S.H.); (631) 632-7928 (B.C.). Fax: (631) 632-6518. E-mail: bhsiao@notes.cc.sunysb.edu (B.S.H.); bchu@notes.cc.sunysb.edu (B.C.).
† Stony Brook University.
‡ Wuhan University.

10.1021/bm061186i CCC: $37.00
Published on Web 05/02/2007

with its manufacturing could be overcome.[8] Due to the serious pollution problems of the viscose method encountered in China, India, and other less-developed countries, the regeneration of cellulose fibers through a new process using low-cost chemical reagents and a simple wet-spinning process with nontoxic byproducts is of great importance. Recently, a new solvent system for cellulose has been demonstrated by the coauthors in China, i.e., NaOH/urea aqueous solution pre-cooled to −10 °C, with which the dissolution of cotton linter pulp could be achieved within about 5 min.[9−11] The cellulose solution could remain in the liquid state for a long period of time at about 0 °C.[9] Experimental cellulose fibers of high quality could be spun from an aqueous solution of 7 wt % NaOH and 12 wt % urea.[10] The relatively low cost and considerably low toxic nature of the NaOH/urea aqueous solution as well as the straightforward wet-spinning procedure all indicate the great potential of using this solvent system for development of an economical and environmentally friendly cellulose fiber fabrication process at an industrial scale.[10]

In this study, the state of aggregation of cellulose molecules in NaOH/urea aqueous solutions has been investigated by static and dynamic light scattering (SLS and DLS). The structural changes in the crystalline region and the corresponding crystal orientations at different processing stages and draw conditions were also characterized by simultaneous wide-angle X-ray diffraction (WAXD) and small-angle X-ray scattering (SAXS). The small beam divergence and the high brilliance of synchrotron X-rays permit measurements with small sample volumes and high spatial resolution.[12] The use of simultaneous SAXS/WAXD has been shown to be particularly powerful for investigating the crystal structure and orientation in polymer materials during processes in real time.[13−17]

Experiments

Cotton linter pulp (degree of polymerization DP ~ 620) was supplied by Hubei Chemical Fiber Co. Ltd. For the fiber spinning study, the cotton linter pulp (e.g., 3.8 g) was dissolved in NaOH (7 wt %)/urea (12 wt %) aqueous solution (e.g., 100 g), precooled at −10 °C, following the procedure demonstrated by Zhang et al.[10,18] This mixture was stirred vigorously for 5 min at room temperature to form a transparent solution as shown in Figure 1. Cellulose solutions at low concentrations (<0.1 wt %) were also prepared for light scattering measurements using the following procedures. The solution was first filtered by an M-size grade glass filter and was kept isothermally at 5 °C for 2 days. To determine the concentration of cellulose in the filtered solution, a stoichiometric amount of 1 M HCl was used to neutralize NaOH. The resulting precipitate was filtered, dried, and weighed. A laser light scattering (LLS) instrument equipped with a BI-9000 AT digital correlator and a solid-state laser (532 nm) was used to determine the molecular conformation of cellulose molecules in NaOH/urea solutions. For static light-scattering, the differential refractive index increment (dn/dc) of the cellulose solution was estimated to be about 0.152 mL/g.[19] The CONTIN program[20] was used for the analysis of the dynamic light-scattering data. The hydrodynamic radius, R_h, was calculated using the Stokes−Einstein relation, $R_h = k_B T/(6\pi\eta D)$, where k_B, T, and η are the Boltzmann constant, the absolute temperature, and the solvent viscosity, respectively, and D represents the translational diffusion coefficient.

A simple laboratory scale wet-spinning apparatus was used to prepare regenerated cellulose fibers, as schematically shown in Figure 2. In this setup, the flow rate of the cellulose solution was controlled by a programmable syringe pump system (Harvard Apparatus). The take-up roller was controlled by a fiber winding device.[13] Only one coagulation bath was used in this setup. The first two cellulose fiber samples (U-1-I and U-1-II) were spun with this apparatus. Their

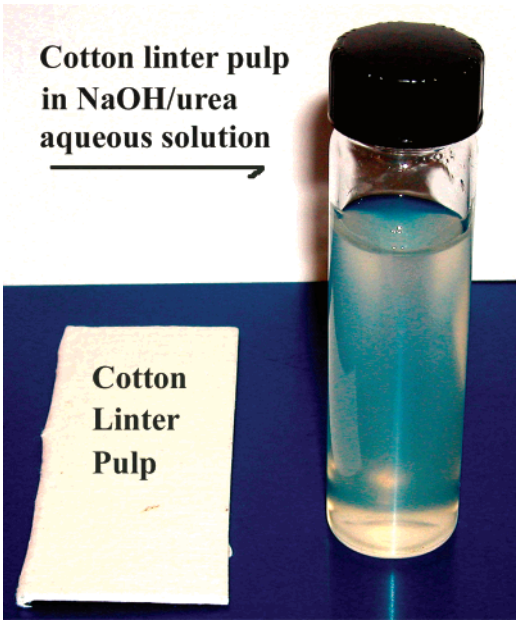

Figure 1. Cotton linter pulp (3.8 wt %) dissolved in 7 wt % NaOH/12 wt % urea aqueous solution.

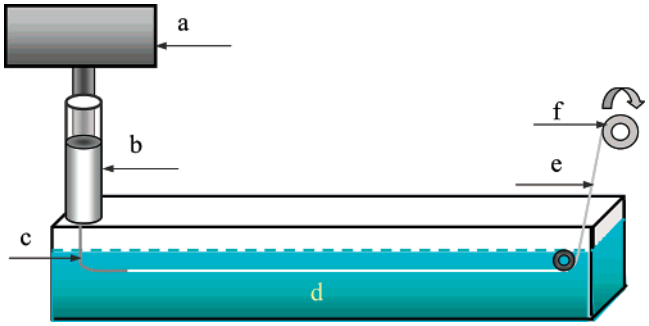

Figure 2. Schematic diagram of a laboratory wet-spinning apparatus: (a) a programmable syringe pump system (Harvard Apparatus); (b) cellulose solution in a syringe (BD 5 mL with slip tip); (c) needle spinneret (BD20G 11/2 precision glide needle, bent into a smooth L-shape); (d) coagulation bath (10 wt % Na_2SO_4 and 15 wt % H_2SO_4 in aqueous solution); (e) cellulose fiber after coagulation; (f) take-up roller, controlled by a polymer fiber spinning apparatus, as shown elsewhere.[12]

spinning conditions are summarized in Table 1. The wet spinning of cellulose solution was also carried out using a pilot wet spinning apparatus equipped with a multi-roller drawing device.[21] With this pilot wet-spinning apparatus, the regenerated cellulose fiber could be drawn at three different stages: (I) first coagulation bath, (II) second coagulation bath, and (III) third post-treatment bath.[21] Three other cellulose fiber samples (U-2-I, U-2-II, and U-2-III) produced at different draw ratios (at different stages) and spinning speeds are also listed in Table 1. Finally, two commercial rayon samples fabricated by the viscose method were also included in this study for comparison. Viscose 1 was supplied by Hubei Chemical Fiber Co., Ltd. Viscose 2 was a precursor for carbon fibers. The surface and cross-section of the regenerated cellulose fibers were examined using scanning electron microscopy (SEM, Hitachi, S-570, Japan), where the surface of the sample was sputtered with gold under vacuum before observation.

Simultaneous wide-angle X-ray diffraction and small-angle X-ray scattering experiments were carried out at the Advanced Polymers Beamline (X27C) in the National Synchrotron Light Source (NSLS), Brookhaven National Laboratory (BNL). A bundle of oriented cellulose fibers was held in the sample holder with the fiber direction perpendicular to the incident X-ray beam. The details of the experimental

Table 1. Coagulation Conditions and Spin Draw Ratio (SDR) Chosen for the Regeneration of Cellulose Fiber in This Study

sample	coagulation bath ($bath_1 \sim bath_2$)	flow speed at spinneret (m/min)	v_I(m/min)/ SDR_I	v_{II}(m/min)/ SDR_{II}	v_{III}(m/min)/ SDR_{III}
U-1-I[a]	10% H_2SO_4/15% Na_2SO_4	2.0	2.0/1	/	/
U-1-II[a]	10% H_2SO_4/15% Na_2SO_4	20.0	20.0/1	/	/
U-2-I	8% H_2SO_4/12% Na_2SO_4 ~ second bath: 4% H_2SO_4	94.8	40.3/0.43	/	/
U-2-II	8% H_2SO_4/12% Na_2SO_4 ~ second bath: 4% H_2SO_4	94.8	40.3/0.43	42.6/1.06	/
U-2-III	8% H_2SO_4/12% Na_2SO_4 ~ second bath: 4% H_2SO_4	94.8	40.3/0.43	42.6/1.06	44.9/1.05

[a] U-1-I and U-1-II were spun by using a laboratory wet spinning instrument as shown in Figure 2; other fibers were wet-spun by using the pilot wet-spun apparatus described in ref 20.

setup at the X27C beamline and the procedures for determining the crystallinity and Hermans' orientation parameter $\bar{P}_{2,g}$ (from the (020) reflection) have been reported elsewhere.[21] The analysis of the equatorial streak in the SAXS patterns was carried out to yield an estimate for the average length of microvoids in cellulose fibers generated at different spinning stages.[22] The procedure is briefly described as follows. If the microvoids are perfectly aligned along the fiber direction and have a uniform finite length, L, then the width of the streak in reciprocal space is independent of the scattering vector ($s = 2 \sin \theta/\lambda$, where 2θ is the scattering angle and λ is the wavelength). Both effects of finite length and orientation can contribute to the width of the equatorial scattering streak. If we assume that these effects can be described by Lorentzian/Cauchy-type functions, then the angular spread (B_{obs}) of the experimental data as a function of s can be given by eq 1, where B_ϕ represents the spread of the misorientation orientation and L is the average length of microvoids.

$$B_{obs} = \frac{1}{L \cdot s} + B_\phi \quad (1)$$

Results and Discussion

Characterization of Cellulose Molecules in NaOH/Urea Aqueous Solutions. It is difficult to truly disperse cellulose molecules in most "known" solvents at the molecular level. For example, based on a light scattering study of polysaccharide solutions, Burchard et al.[23] suggested that even after full dissolution, there still remained a fringed-micelle like molecular superstructure in most systems. The aggregation of cellulose molecules in viscose and NMMO-based solution has also been widely reported.[23−26] For example, Seger and Fischer investigated the viscose solution after dilution in 1 M NaOH by static light scattering[24,25] and gave an aggregation number around 10 laterally assembled chains.[25] The radius of gyration R_g (266 nm) of such a structure was much larger than that of the molecularly dispersed cellulose chains (57 nm). Röder et al. also studied the cellulose molecules in NMMO using the same technique and reported an R_g value of about 200 nm.[26]

In this study, the aggregation behavior of cellulose molecules in the NaOH/urea aqueous solutions was investigated by combined static and dynamic laser light scattering. It was found that the state of aggregation was not sensitive to slight variations of solvent mixtures or preparation conditions. The light scattering experiments were repeated several times, and the results were reproducible. It was found that the cellulose molecules in the NaOH/urea aqueous solution formed aggregates and exhibited typical R_g values in the range of 200 to 300 nm, which are comparable to those obtained in other solvent systems. Figure 3A shows the Zimm plot of the cellulose molecules in 7 wt % NaOH/12 wt % urea aqueous solution at 25 °C. The cellulose aggregates in this solution exhibited an R_g value of 232 nm

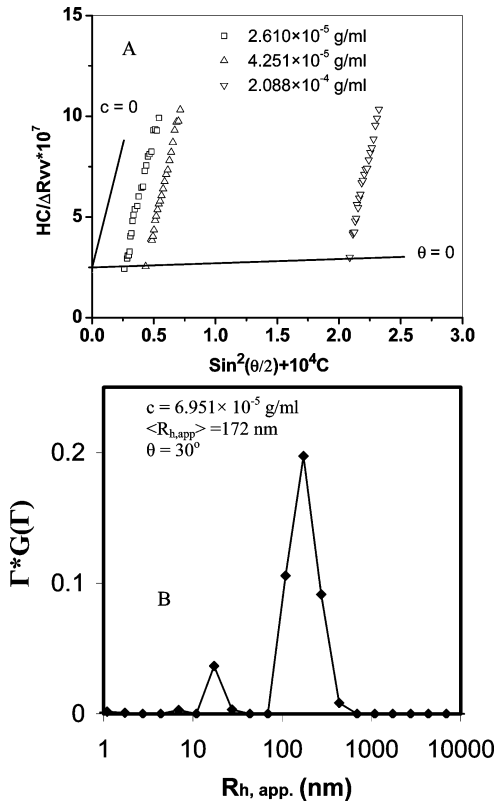

Figure 3. (A) Zimm plot of cellulose in 7 wt % NaOH/12 wt % urea aqueous solution at 25 °C. (B) The CONTIN analysis of DLS measurements on cellulose solutions. $\Gamma^*G(\Gamma)$ denotes the fraction of scattered intensity over the line-width range with $R_h = k_B T/(6\pi\eta D)$ and $\Gamma = Dq^2$.

and a molecular weight (M_w) of 4.07×10^6 g/mol. Both values are significantly higher than those of cellulose molecules in the 6 wt % NaOH/4 wt % urea aqueous solution (R_g of 50 nm and M_w of 1.1×10^5 g/mol).

Dynamic light scattering (DLS) results indicated that the cellulose molecules in 7 wt % NaOH/12 wt % urea aqueous solution had an average hydrodynamic radius R_h of about 165 nm. Figure 3B shows a typical apparent hydrodynamic radius distribution as obtained by the CONTIN analysis at different cellulose concentrations in the dilute solution regime. The dominant second maximum around $R_h = 172$ nm was too large for a single cellulose chain and thus represented an aggregated state of the cellulose molecules. These results yielded an R_g/R_h ratio of about 1.4 ($R_g = 232$ nm and $R_h = 165$ nm), which is in the range for polymer coils as discussed by Burchard et al.[23] The size of the cellulose aggregates in NaOH/urea aqueous solution is similar to that in the viscose solutions ($R_g = 266$

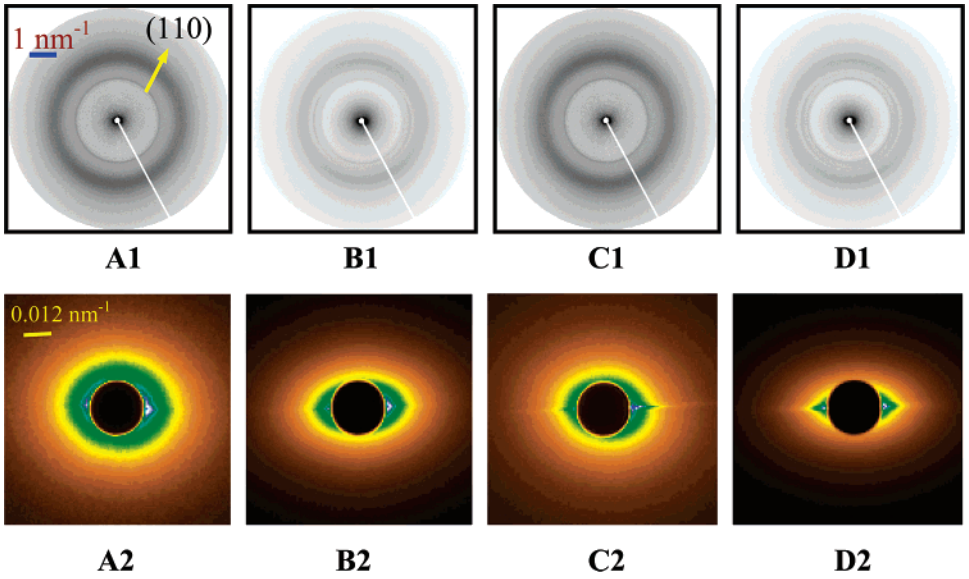

Figure 4. WAXD/SAXS patterns of cellulose gel fibers and wet fibers at different flow rates. (A1/A2) and (B1/B2) represent the gel fiber and wet fiber at a flow rate of 2 m/min; (C1/C2) and (D1/D2) represent the gel fiber and wet fiber at a flow rate of 20 m/min.

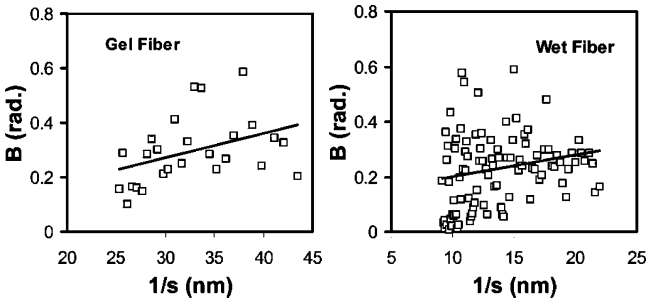

Figure 5. Integral breadth of equatorial streak (*B*) vs 1/*s* from the SAXS patterns (C2 and D2 in Figure 3) of the gel fiber (or coagulated fiber) and wet fiber.

nm) with a similar cellulose molecular weight.[26,27] Thus, the NaOH/urea solvent mixture exhibited a comparable behavior to the viscose solvent system, i.e., both systems could not truly dissolve the cellulose molecules at the molecular level.

The dissolution behavior of cellulose in NaOH/urea aqueous solution is very different from that in aqueous NaOH solution without urea. The polar amine and carbonyl groups of urea could be considered as hydrogen-bonding donors and acceptors, respectively, for the cellulose molecules.[28] The presence of NaOH produces ion-pair interactions, which can reduce the strong self-association character of water, allowing hydrogen bonds to be formed between urea and cellulose.[28] These intermolecular interactions in the NaOH/urea solvent should facilitate the dissolution of cellulose. However, as the dissolution time in our study was relatively short (about 5 min), not all the hydrogen bonds between the cellulose chains could be broken. The observed aggregates probably still consisted of cellulose chains bonded together by hydrogen bonds. We hypothesize that the dissociation of molecular aggregates into single chains would be a very slow process. More experimental results need to be carried out to verify this hypothesis.

Upon solidification during fiber spinning, the cellulose chains were found to exclusively crystallize into the cellulose II crystal structure, having an antiparallel chain configuration. The cellulose I structure with a parallel chain configuration, typically found together with the cellulose II structure in native cellulose, was not observed. Kim et al. have recently studied the transformation of the parallel chain configuration in cellulose I to the antiparallel chain configuration in cellulose II during the mercerization process.[29] Using dark field and electron diffraction techniques in transmission electron microscopy (TEM), they concluded that an intermingling of the cellulose chains from neighboring microfibrils of opposite polarity could play an important role in this transformation.[29] It is conceivable that the cellulose chains, initially dispersed in NaOH/urea aqueous solution as aggregates, can undergo a sequential structural change during the solidification step from metastable cellulose I to the more thermodynamically stable cellulose II. The molecular aggregation behavior thus not only influences the rheological properties of the solution but also affects the structure and property relationships of the regenerated cellulose fiber.

Structure Development of Cellulose Fibers at Different Spinning Stages and Different Flow Rates. The structure development of the regenerated cellulose fibers at different spinning stages during wet spinning was systematically studied. When the cellulose solution was immersed in the coagulation bath, the fast ion exchange and neutralization processes resulted in quick gelation, forming a gel-like fiber (termed 'gel fiber' hereafter). Figure 4 shows the WAXD/SAXS patterns of cellulose fibers obtained at different wet spinning stages. The WAXD patterns of the fibers after coagulation (A1 and C1 gel fibers) and washing (B1 and D1 wet fibers) were very similar; both exhibited a diffraction peak close to the (110) reflection of the cellulose II crystal structure. The strong halo around $s = 3.3$ nm^{-1} from the gel fiber (pattern A1) might be attributed to a cellulose−sodium ion complex, which will be the subject of future investigation. This maximum moved to around $s = 3.1$ nm^{-1} after washing in the wet fiber (pattern B1). Figure 4 clearly shows the absence of crystalline cellulose regions after coagulation and washing, indicating that these fibers consisted of a poorly ordered structure of hydrated cellulose chains held together by hydrogen bonds at the initial stage of wet-spinning. A 3D cellulose crystal structure would only develop upon drying of the sample.

The anisotropic equatorial streaks in the SAXS patterns (Figure 4 patterns A2−D2) indicate that the cellulose fibrils

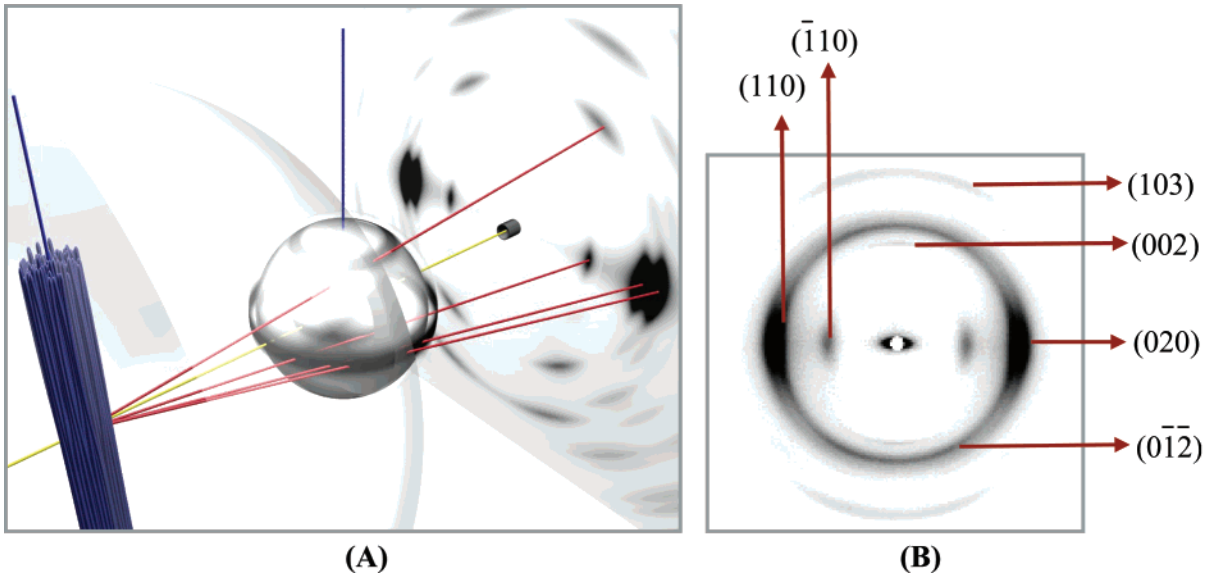

Figure 6. (A) Schematic visualization of 2D fiber diffraction pattern for the cellulose II structure. (B) Typical 2D WAXD pattern measured from the regenerated cellulose fiber (U-2-III); all observed reflection peaks could be indexed by the cellulose II structure.

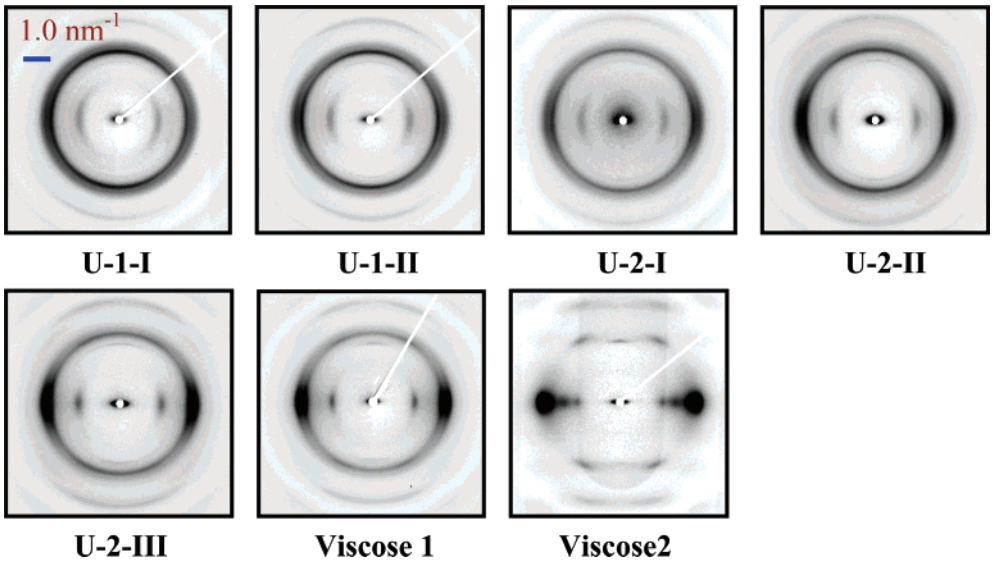

Figure 7. WAXD patterns of cellulose fibers spun from the NaOH/urea aqueous solution and commercial viscose rayon fibers.

are extended and oriented after gelation. This suggests that some fibrillar superstructure is formed at the initial stages of the wet spinning. In 1956, Statton proposed that the diffuse equatorial streak feature in SAXS from cellulose fibers could be mainly attributed to the presence of microvoids, elongated parallel to the fiber axes.[30] Hermans, Heikens, and Weidinger investigated the diffuse SAXS pattern of cellulose fibers and estimated the volume fraction of microvoids, which was about 1% in a solid matrix.[31,32] Perret and Ruland further demonstrated an advanced quantitative technique to determine the microvoid structure in this type of fibers.[33] In Figure 4, it is interesting to notice that the equatorial streak in SAXS was relatively weak (e.g., patterns A2 and B2) at low flow rates (e.g., 2 m/min); while the equatorial streak became very strong (e.g., patterns *C*2 and D2) at high flow rate (e.g., 20 m/min). It is conceivable that at low flow rates, the microvoids were filled with water, lowering the density contrast in SAXS; whereas at higher flow rate, the water infiltration into the microvoids may be incomplete, leading to a larger density contract to enhance the scattered intensity.

Figure 5 shows the dependence of the angular integral breadth of the equatorial streak (B) on the reciprocal scattering vector 1/*s* for both gel and wet fibers (the wet fiber was spun at a flow rate of 20 m/min, corresponding to the SAXS patterns C2 and D2 in Figure 4). On the basis of eq 1, the estimated lengths of the microvoids were about 115 and 128 nm for the gel and wet fibers, respectively. The average length of the microvoids of the wet fiber was slightly larger than that of the gel fiber, possibly due to the removal of ions from the gel fiber.

WAXD/SAXS Characterization of Regenerated Cellulose Fibers. Simultaneous SAXS and WAXD measurements were used to characterize the structure and morphology of the regenerated cellulose fibers spun from the NaOH/urea aqueous solution. Figure 6A shows a schematic diagram of the scattering experiment leading to the 2D WAXD pattern of a bundle of fibers with cellulose II crystal structure, where the bundles with preferred orientation (blue), primary beam (yellow), scattered beams (red), translucent Ewald sphere, translucent pole figures with equatorial belts for the (*hk*0) reflections and non-equatorial

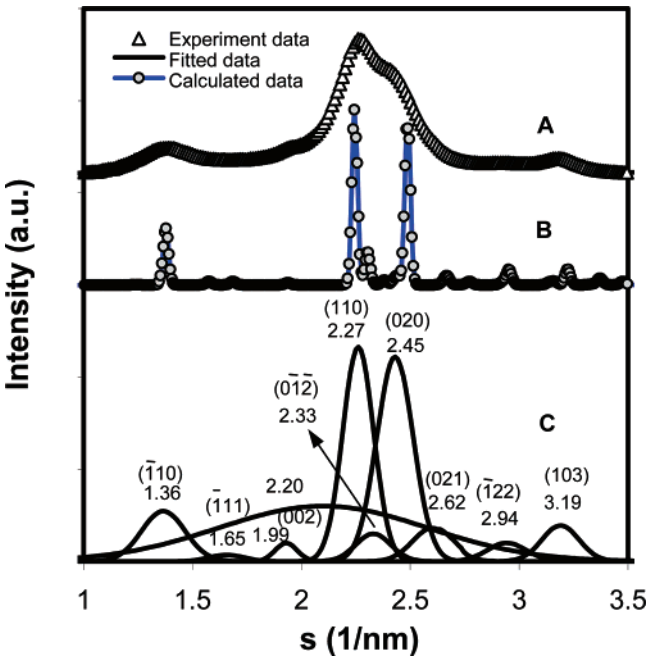

Figure 8. One-dimensional integrated WAXD intensity profile of the viscose 1 sample and the corresponding peak separation analysis to estimate the crystallinity and crystal size: (A) experimental intensity profile, (B) calculated intensity profile based on the cellulose II structure, and (C) the nine crystal reflections and the amorphous background.

rings for the (0 $\bar{1}$ $\bar{2}$) reflection, 2D detector with beam stop, and corresponding 2D WAXD pattern are illustrated. The detected intensity corresponds to the intersection of the Ewald sphere with the (*hkl*) intensity pole figures. A typical 2D WAXD pattern from the U-2-III sample (its processing conditions are listed in Table 1) is shown in Figure 6B, where all reflections can be indexed based on the known cellulose II crystal structure with a monoclinic unit cell and lattice constants of $a = 8.10$ Å, $b = 9.03$ Å, $c = 10.31$ Å, and $\gamma = 117.1°$ as reported by Langan et al.[34] This confirms that the cellulose I structure present in native cotton linter pulp was completely transformed; only the cellulose II structure was produced after spinning from the NaOH/thiourea solution. Figure 6 also shows that the (110), ($\bar{1}$10), and (020) reflections are located on the equator, while non-(*hk*0) reflections are located at the off-axis positions. This indicates that, in these regenerated fibers, the cellulose II structure was preferentially oriented with its crystallographic *c*-axis pointing in the fiber direction.

Figure 7 shows 2D WAXD patterns of all cellulose fiber samples prepared in this study as well as of three commercial rayon fiber samples. It is seen that all regenerated fibers exhibited the cellulose II structure. The first three WAXD patterns (U-1-I, U-1-II, and U-2-I) were very similar to each other—their reflections all appeared as broad arcs, indicating the presence of moderate crystal orientation. However, the reflections of the WAXD pattern in the U-2-III exhibited narrow equatorial arcs, which were close to those in viscose 1 indicating a high degree of crystal orientation. (We note that the orientation of our regenerated fibers was always lower than that of viscose 1 because the chosen spinning/drawing conditions were not yet optimized.)

The procedures for determining crystallinity and crystal size from the WAXD data are illustrated in Figure 8. In brief, an example integrated intensity profile (Figure 8A) was obtained by spherical averaging of the Fraser-corrected[35] 2D WAXD pattern. On the basis of this intensity profile from the cellulose II structure (Figure 8B), nine crystal reflection peaks were used to fit the data (Figure 8C). The amorphous scattering background was obtained from the WAXD measurement of ball-milled as-spun cellulose fibers, containing only the amorphous phase. The crystallinity and lateral crystal size (that are related to the crystal fibril diameter) of regenerated cellulose fibers are listed in Table 2. It was found that the total crystallinity of regenerated cellulose fibers prepared in this study was higher than that of viscose 2. The crystal sizes of regenerated cellulose fibers were also larger than the typical values of viscose rayon fibers. It is known that many factors can affect the crystallinity and crystal size of regenerated cellulose fibers through wet spinning. On the basis of the results from U-2-I, U-2-II, and U-2-III samples (which experienced a similar wet-spinning condition), we conclude that both crystallinity and crystal size were increased after the second coagulation stage, when compared to the values after the first coagulation stage. However, a decrease of the crystal size in the third post-treatment bath was also observed, which can be explained by the chain pull-out from the crystal regions at high draw ratios.

Table 2. Crystallinity, Orientation Parameter, and Length of Microvoids in the Regenerated Cellulose Fibers in This Study and from Other Commercial Sources

sample	total crystallinity (%)	crystal size (nm)	Hermans' orientation parameter	microvoids length *L* (nm)
U-1-I	58	5.31	0.42	114
U-1-II	60.5	5.70	0.51	161
U-2-I	57	5.76	0.56	476
U-2-II	59	6.10	0.57	619
U-2-III	61	5.59	0.64	1250
viscose 1	58	5.32	0.68	625
viscose 2	49.1	4.99	0.90	2000

Table 3. Calculated Values of Isotropic Fraction (p0), Orientation Parameter (*p*), and Hermans' Orientation Parameter ($\bar{P}_{2,g}$) of the Regenerated Cellulose Fibers Using Eq 2

sample	p_0	p	$\bar{P}_{2,g}$
U-1-I	0.42	10	0.42
U-1-II	0.37	15	0.51
U-2-I	0.32	16	0.56
U-2-II	0.135	17	0.57
U-2-III	0.30	34	0.64
viscose 1	0.27	40	0.68
viscose 2	0.07	95	0.90

In regenerated cellulose fibers, the crystal orientation plays an important role in affecting the mechanical properties. Table 2 lists Hermans' orientation parameter[21] calculated from the (020) reflection in the 2D WAXD patterns. The values of Hermans' orientation parameter, $\bar{P}_{2,g}$, of regenerated cellulose fibers U-1-I was only 0.42, which was lower than those of other regenerated cellulose fibers. This was probably due to the application of a very low flow rate during wet spinning (Table 1). The $\bar{P}_{2,g}$ value of U-1-II was much higher than that of U-1-I, which confirmed the notion that the higher flow rate results in higher crystal orientation. For U-2-I, U-2-II, and U-2-III samples, Hermans' orientation parameter was found to increase with the draw ratio at all postprocessing stages, but especially notable after the third treatment bath. Due to the high crystal orientation, the mechanical properties of U-2-III were also found to be close to those of commercial viscose 1 fibers.[11] The Hermans' orientation parameters of crystal structures from

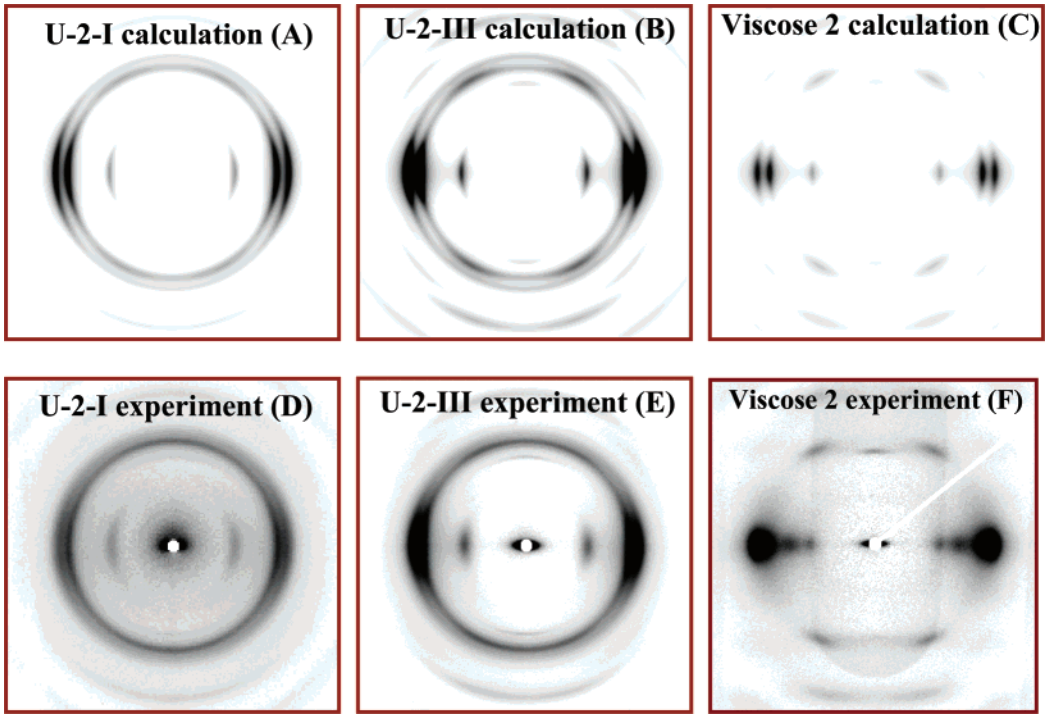

Figure 9. Two-dimensional fiber diffraction patterns of the cellulose II structure from experiment and calculation.

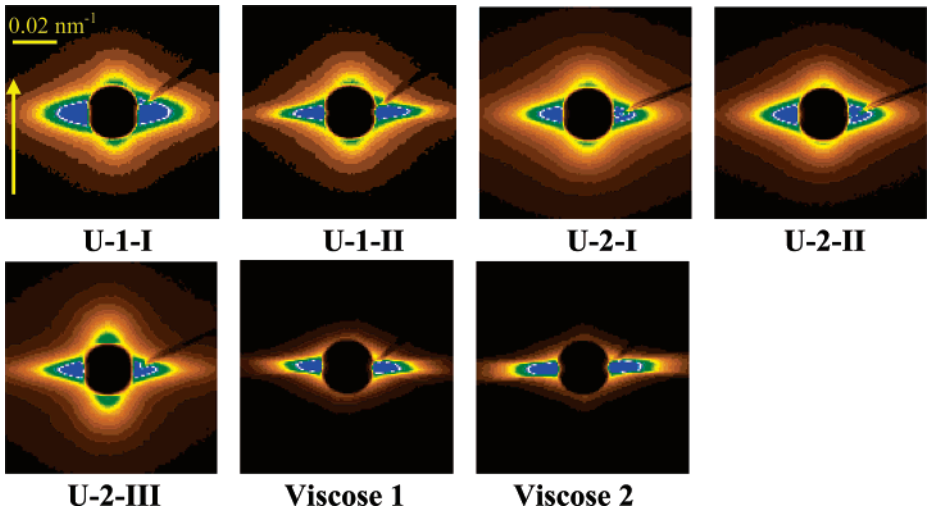

Figure 10. Two-dimensional SAXS pattern of the cellulose fibers (the arrow inset in U-1-I shows the fiber direction).

viscose1 and viscose 2 fibers determined in this study were all quite high, e.g., around 0.9 for the viscose 2 fiber.

Instead of reducing the distribution of crystal orientation to a single parameter $\bar{P}_{2,g}$, we also used the orientation distribution function $g(\beta)$ to describe the observed orientation, where β is the angle between the fiber axis and the *c*-axis of an oriented crystallite. Using the modified Onsager orientation distribution from ref 20, an isotropic fraction p_0 and an orientation parameter p, the parameter $\bar{P}_{2,g}$ can be expressed as follows.[21]

$$\bar{P}_{2,g} = (1 - p_0)\{1 - 3p^{-1}[\coth(p) - p^{-1}]\} \qquad (2)$$

The comparison of the calculated 2D fiber diffraction patterns and the experimental patterns is shown in Figure 9, where a very good agreement was seen between the two sets. Figures 9A and 9B show the calculated fiber diffraction patterns for samples U-2-I (Figure 9D) and U-2-III (Figure 9E). The isotropic fraction $p_0 = 0.32$ and an orientation parameter $p = 16$ (resulting in a $\bar{P}_{2,g}$ of 0.56) were used to calculate the pattern in Figure 9A. The calculated $\bar{P}_{2,g}$ value matches well with that determined from the experimental U-2-I pattern (Figure 9D). An isotropic fraction $p_0 = 0.30$ and orientation parameter $p = 34$ were used for calculation in Figure 9B, leading to a Hermans' orientation parameter $\bar{P}_{2,g}$ of 0.64. A well-oriented ($p = 95$) cellulose II fiber structure with a very small isotropic fraction ($p_0 = 0.07$) corresponding to $\bar{P}_{2,g} = 0.90$ was used to approximate the viscose 2 pattern as shown in Figure 9C.

The values of the isotropic fraction p_0 and the orientation parameter p can give some insights into the composition of the regenerated cellulose fiber. Table 3 lists the calculated values of the isotropic fraction p_0 and the orientation parameter p for all regenerated cellulose fibers and viscose rayon fibers used in this study. Comparing results from U-1-I and U-1-II samples, we conclude that the increase in flow rate (from 2 m/min (U-

1-I) to 20 m/min (U-1-II)) resulted in a large increase in orientation parameter (p), a decrease in isotropic fraction (p_0), and an increase in Hermans 'orientation parameter (from 0.42 to 0.51). For the U-2-I, U-2-II, and U-2-III samples prepared by the pilot spinning apparatus using a high spinning speed (94.8 m/min) and multi-roller drawing steps, the isotropic fraction decreased only slightly (from 0.32 for U-2-I to 0.30 for U-2-III); however, the orientation parameter p increased noticeably (from 16 for U-2-I to 34 for U-2-III). This indicates that the draw processing significantly increased the orientation in regenerated cellulose fibers. Furthermore, the calculated values of the isotropic fraction p_0 and the orientation parameter p for U-2-III were close to those of the viscose 1 fiber, indicating that the orientation in regenerated cellulose fibers could be improved to a level similar to that of commercial rayon fibers. Both viscose 1 and viscose 2 fibers exhibited small p_0 and large p values, again indicating a very high degree of orientation in the crystalline domains.

Figure 10 shows the observed SAXS patterns of the regenerated cellulose fibers investigated in this study (Table 1) as well as of the viscose 1 and viscose 2 samples. For all regenerated cellulose fibers, the scattering pattern showed a sharp and elongated equatorial streak superimposed with a relatively weak and short meridional intensity distribution. However, only a sharp and elongated equatorial streak was seen in viscose 1 and viscose 2 fibers. As discussed above, the equatorial streak can be mainly attributed to the existence of microvoids, where the amount of microvoids is strongly dependent on the spinning conditions. The elongated shape of the equatorial streak indicated that the microvoids were needle-shaped and aligned parallel to the fiber direction.

Table 2 revealed several interesting features. (1) The length of microvoids in U-1-1 was 114 nm and in U-1-2 was 161 nm, indicating that the length of microvoids increases with the wet spinning flow rate. In other words, the high flow rate can not only orient the cellulose chains but also elongate the microvoids. (2) The draw ratio also affected the length of the microvoids. For example, in the samples U-2-I, U-2-II, and U-2-III, the draw ratio in the second coagulation bath and third post-treatment bath significantly increased the length of microvoids. The length of the microvoids in viscose 2 was quite long (about 2 μm), probably indicating an extensive drawing process.

The appearance of meridional scattering peaks in SAXS from the regenerated cellulose fibers suggested the presence of periodic lamellar structure between the crystalline and amorphous regions. The long period, representing the average distance between the adjacent crystalline lamellae, could be estimated from the position of the meridional scattering maximum, but was found to be outside our current experimental range, i.e., larger than 100 nm. Fischer et al. have also reported the appearance of discrete meridional peaks in rayon fibers using small-angle neutron scattering (SANS).[36] It is not clear why their long period was much shorter than ours, perhaps this is because of the different flow conditions and solution properties involved.

Morphology and Mechanical Properties of Regenerated Cellulose Fibers. We note that regenerated cellulose fibers prepared by the new NaOH/urea aqueous solution system exhibited a high-quality appearance with uniform surface morphology and good mechanical properties similar to those of commercial rayon fibers.[11] Specifically, the dried regenerated cellulose fibers always showed a smooth circular cross-section, which was very different from the irregular shape of cross-sections from viscose rayon fibers but was similar to those of cuprammonium rayon and Lyocell fibers.[37−38] Because of the round shape and uniform surface structure, the regenerated cellulose fiber has an excellent feel, bright appearance, and good mechanical properties (e.g., tensile strength of 1.9 cN/dtex), even when prepared under different spinning conditions.

Conclusions

Synchrotron X-ray diffraction and scattering techniques were used to characterize regenerated cellulose fibers prepared from an environmentally friendly NaOH/urea aqueous solution. Light scattering results showed that cellulose molecules in the 7 wt % NaOH and 12 wt % urea aqueous solution formed molecular aggregates having a radius of gyration R_g of about 230 nm, which is in agreement with that in the typical viscose solution of similar cellulose molecular weight. SAXS results indicated the presence of dominant microvoids and fibrillar structure induced by spin−draw processes in both gel and wet fibers. Although crystallinity, crystal size, and crystal orientation of regenerated cellulose fibers varied under different postprocessing conditions, only the cellulose II crystal structure was observed. At high flow rates and high draw ratios (i.e., by the multi-roller drawing process), the crystal orientation of regenerated cellulose fibers became significantly higher. Finally, we note that the chosen solvent system, its byproducts, and resulting fibers are all free of sulfur, contrary to the viscose rayon process. The new solvent system thus may offer a practical alternative with lower cost potential and improved environmental friendliness over the existing methods for production of high-quality cellulose fibers.

Acknowledgment. The financial support of this work was provided by the Department of Energy (DEFG0286ER45237.023 and DEFG0299ER45760) and the National Science Foundation (DMR0454887 and DMR0405432). L.Z. gratefully acknowledges the support of this work by the National High Technology Research and Development Program of China (2003AA333040) and the National Natural Science Foundation of China (59933070).

Supporting Information Available. SEM images of viscose rayon, cuprammonium rayon, Lyocell fiber, and the new regenerated cellulose fiber (U-2-III). This material is available free of charge via the Internet at http://pubs.acs.org.

References and Notes

(1) Mohanty, A. K.; Misra, M.; Drzal, L. T. *J. Polym. Environ.* **2002**, *10*, 19.
(2) Helbert, W.; Cavaille, J. Y.; Dufresne, A. *Polym. Compos.* **1996**, *17*, 604.
(3) Fisher, G. *Int. Fiber J.* **1999**, *14* (5), (http://www.ifj.com/issue/october99/4.html).
(4) Fink, H. P.; Weigel, P.; Purz, H. J.; Ganster, J. *Prog. Polym. Sci.* **2001**, *26*, 1473. Zugenmaier, P. J. *Prog. Polym. Sci.* **2001**, *26*, 1341.
(5) Philipp, B. *J. Macromol. Sci., Pure Appl. Chem.* **1993**, *A30*, 703.
(6) Okubayashi, S.; Bechtold, T. *Cellulose* (Dordrecht, Netherlands), **2005**, *12*, 459.
(7) Rosenau, T.; Potthast, A.; Sizta, H.; Kosma, P. *Prog. Polym. Sci.* **2001**, *26*, 1837.
(8) Vargas, E. *Spunlace Technology Today: An Overview of Raw Materials, Processes, Products, Markets and Emerging End Uses*; Miller Freeman Publications: San Francisco, CA, 1989; p 61.
(9) Cai, J.; Zhang, L. *Biomacromolecules* **2006**, *7*, 183.
(10) Cai, J.; Zhang, L.; Zhou, J.; Li, H.; Chen, H.; Jin, H. *Macromol. Rapid Commun.* **2004**, *25*, 1558.
(11) Cai, J.; Zhang, L.; Zhou, J.; Qi, H.; Chen, H.; Kondo, T.; Chen, X.; Chu, B. *Adv. Mater.* In press.
(12) Chu, B.; Hsiao, B. S. *Chem. Rev.* **2001**, *101* (6), 1727.

(13) Ran, S.; Burger, C.; Fang, D.; Zong, X.; Cruz, S.; Chu, B.; Hsiao, B. S.; Bubeck, R. A.; Yabuki, K.; Teramoto, Y.; Martin, D. C.; Johnson, M. A.; Cunniff, P. M. *Macromolecules* **2002**, *35*, 433.
(14) Chen, X.; Burger, C.; Wang, X.; He, W.; Yoon, K.; Somani, R. H.; Fang, D.; Sics, I.; Rong, L.; Hsiao, B. S.; Chu, B. *Macromolecules* **2006**, *39*, 5427.
(15) Kelarakis, A.; Yoon, K.; Somani, R. H.; Chen, X.; Hsiao, B. S.; Chu, B. *Polymer* **2005**, *46*, 11591.
(16) Liu, L.; Wan, Q.; Liu, T.; Hsiao, B. S.; Chu, B. *Langmuir* **2002**, *18*, 10402.
(17) Chen, X.; Yoon, K.; Burger, C.; Sics, I.; Fang, D.; Hsiao, B. S.; Chu, B. *Macromolecules* **2005**, *38*, 3883.
(18) Zhang, L.; Cai, J.; Zhou, J. ZL 03128386.1, 2005.
(19) Zhou, J.; Zhang, L.; Cai, J. *J. Polym. Sci., Part B: Polym. Phys.* **2004**, *42*, 347.
(20) Chu, B. *Laser Light Scattering*, 2nd ed.; Academic Press: New York, 1991.
(21) Chen, X.; Burger, C.; Fang, D.; Hsiao, B. S.; Chu, B. *Polymer* **2006**, *47*, 2839.
(22) Ruland, W. *J. Polym. Sci., Part C: Polym. Lett.* **1969**, *28*, 143.
(23) Schulz, L.; Seger, B.; Buchard, W. *Macromol. Chem. Phys*. **2000**, *201*, 2008.
(24) Seger, B. Ph.D. Thesis 1996, University of Freiburg.
(25) Fischer, K. *Papier* **1994**, *48*, 769.
(26) Morgenstern, B.; Röder, T. *Papier* **1998**, *52*, 713.
(27) Röder, T. Ph.D. Thesis 1998, Technical University of Dresden.
(28) Zhang, L.; Ruan, D.; Zhou, J. *Ind. Eng. Chem. Res.* **2001**, *40*, 5923.
(29) Kim, N. H.; Mai, T.; Wada, M.; Sugiyama, J. *Biomacromolecules* **2006**, *7*, 274.
(30) Statton, W. O. *J. Polym. Sci.* **1956**, *32*, 395.
(31) Hermans, P. H.; Heikens, D.; Weidinger, A. *J. Polym. Sci.* **1959**, *35*, 145.
(32) Heikens, D. *J. Polym. Sci.* **1959**, *35*, 139.
(33) Perret, R.; Ruland, W. *J. Appl. Crystallogr.* **1969**, *2*, 209.
(34) Langan, P.; Nishiyama, Y.; Chanzy, H. *Biomacromolecules* **2001**, *2*, 410.
(35) Ran, S.; Wang, Z.; Burger, C.; Chu, B.; Hsiao, B. S. *Macromolecules* **2002**, *35*, 10102.
(36) Fischer, E. W.; Herchenroder, P.; Manley, R. St. J.; Stamm, M. *Macromolecules* **1978**, *11*, 213.
(37) Woodings, C. *Regenerated Cellulose Fibres*; Woodhead Publishing Ltd: England, 2001.
(38) Ziabicki, A. *Fundamentals of Fiber Formation*; John Wiley and Sons: London, 1976.

BM061186I